Approximate Analysis of the Slot Injection of a Gas in Laminar Flow

PAUL A. LIBBY* AND JOSEPH A. SCHETZ†
General Applied Science Laboratories Inc., Westbury, N. Y.

The laminar diffusion and combustion of a gas injected into a high-speed uniform stream by means of a wall slot are considered. The Dorodnitzin-Howarth transformation is employed to reduce the boundary layer equations to incompressible form; the nonsimilar flow field is treated by a modified Oseen approximation in conjunction with the integral method. Thermal boundary conditions corresponding to an adiabatic wall and to constant wall enthalpy are discussed. The injection of homogeneous, heterogeneous, nonreactive, and reactive gases is treated. For the latter case, the models usually employed for chemical behavior, namely, frozen and equilibrium flow, are considered. The analysis is applicable to a wide variety of laminar flows, e.g., those involving cooling, thermal protection, skin-friction reduction, and supersonic deflagration. A numerical example of practical interest in connection with the venting of gaseous hydrogen boiloff from a rocket booster is presented.

Nomenclature

a = slot height in physical coordinates
$A(\xi)$ = function defined by Eq. (7)
$B(\xi, \xi_1)$ = function defined by Eq. (15a)
C = Chapman constant
C_f = skin friction coefficient = $\tau_0/\rho_e u_e^2$
g = stagnation enthalpy nondimensionalized with freestream conditions
h = enthalpy
$\mathfrak{h}$ = heat transfer coefficient based on enthalpy
k = thermal conductivity
Le = Lewis number
Nu = Nusselt number = $\mathfrak{h}x/(k/C_p)_w$
Re = Reynolds number = $\rho_e u_e x/\mu_e$
= transformed normal coordinate
t_a = transformed slot height
T = temperature
u = streamwise velocity
$\tilde{u}$ = u/u_e = streamwise velocity nondimensionalized with freestream conditions
W = molecular weight
x = streamwise coordinate
$\tilde{x}$ = x/t_a = nondimensional streamwise coordinate
$\bar{x}$ = $(x/t_a)(C\mu_e/\rho_e u_e t_a)$ = nondimensional streamwise coordinate
y = normal coordinate
Y_i = mass fractions
$\hat{Y}_i$ = element mass fractions
θ = momentum thickness
$\tilde{\theta}$ = θ/t_a = nondimensional momentum thickness
Θ = $(T - T_r)/(T_e - T_r)$ = nondimensional temperature ratio
μ = viscosity
ξ_1 = velocity length variable
ξ_2 = energy length variable
σ = Prandtl number
ρ = density
τ = t/t_a = nondimensional transformed normal coordinate
Ω = energy thickness
$\tilde{\Omega}$ = Ω/t_a = nondimensional energy thickness

Subscripts

e = freestream conditions
f = conditions at flame sheet
j = conditions at slot inlet ($x = 0$)
r = reference conditions
s = stagnation conditions
w = conditions at the wall
1 = oxygen
2 = hydrogen
3 = water
4 = nitrogen

I. Introduction

THE influence of mass transfer on boundary layer properties has been the subject of intensive study in the past.[1-3] Most studies have been concerned with distributed injection as occurs over porous and/or ablating surfaces. The problem considered here is the case of tangential injection by means of a wall slot as depicted schematically in Fig. 1. This flow is of present interest in several applications, for example, as a fuel injection system for air-breathing engines employing supersonic deflagration-type combustion as proposed by Ferri.[4] This manner of fuel injection might be of particular importance, since it can provide gaseous film cooling for internal engine surfaces as well as an effective means of fuel injection and mixing. The high heat transfer where the reaction zone approaches the wall can be avoided by successive slots. A second direct application of this study is to the problems associated with the venting of liquid propellant boiloff from rocket boosters at high altitudes. In addition, the slot injection of reactive or nonreactive gases is of interest in connection with the cooling of exposed surfaces, reducing skin-friction, and providing thermal protection. Under high-altitude hypersonic flow conditions, these applications often involve laminar flow.

In the analysis presented here the following idealizations are employed. The flow is considered laminar, steady, and two-dimensional. The pressure is taken to be constant throughout. The profiles of velocity, composition, and temperature at the origin of mixing ($x = 0$) are considered uni-

Received by ARS August 3, 1962; revision received February 25, 1963. This research was carried out under Contract No. AF 49(638)-991 with the Office of Scientific Research of the Air Research and Development Command. Technical monitoring was done by Milton M. Slawsky, Director, Aeronautical Sciences, Air Force Office of Scientific Research. This paper received limited distribution in an extended form and under slightly modified title as Air Force Office of Scientific Research, General Applied Science Labs. TR 229, "Approximate analysis of slot injection of a reactive gas in laminar flow" (June 1962). The authors are pleased to acknowledge that Antonio Ferri suggested the problem considered herein, that Leatrice Groffman carried out the numerical computations, and that Frank Lane provided helpful suggestions.

* Senior Scientific Investigator; also Professor of Aerospace Engineering, Polytechnic Institute of Brooklyn, Brooklyn, N. Y. Member AIAA.
† Senior Scientist.

form so that the influence of the boundary layers on the wall ($y = 0$) and on the splitter plate ($y = a$) for $x \leq 0$ is neglected. The chemical behavior in the case of reactive gases is taken to correspond to frozen flow and to equilibrium chemistry as approximated by a flame sheet.[2] The chemical system studied in detail is that of hydrogen injected into an airstream. The Prandtl number and all Lewis numbers are taken to be unity.

Although the much more complicated problems of turbulent flow and nonequilibrium chemistry are of great interest, the simplifying assumptions adopted herein leave wide areas of practical application. For example, hypersonic air-breathing vehicles operating at high altitudes would have inlet conditions of very high static temperature and low static pressure which would result in laminar flow and near-equilibrium chemical behavior.

The flow resulting from slot injection is, in general, of the nonsimilar type involving the initial value problem of boundary layer theory. Consequently, there are available the finite difference methods of computation,[5-7] the strip method of Pallone,[8] or the more approximate techniques based on integral methods using polynomial profiles.[9-11] The more exact methods involve considerable computational complexity, whereas the previously employed integral methods have limited freedom in the initial profiles that can be represented. In this report a new adaption of the modified Oseen method of Carrier and Lewis[12] and of Carrier[13] is employed to yield a simple approximate solution based on the integral method with profiles generated by a solution to a related heat conduction equation. This approach provides a general method of approximate solution for all nonsimilar viscous flow problems.

II. Analysis of the Velocity Field

Consider first the velocity distribution associated with the general physical problem shown in Fig. 1. The compressible flow problem can be transformed into a corresponding incompressible flow by introducing the Dorodnitzin-Howarth variable t, defined by

$$t = \int_0^y \frac{\rho}{\rho_e}\, dy \tag{1}$$

With the assumption[14] $\rho_w\mu_w/\rho_e\mu_e = C(x)$, the nondimensional integral momentum equation in the incompressible plane can written

$$\frac{d\tilde{\theta}}{d\tilde{x}} = \frac{C\mu_e}{\rho_e u_e t_a}\left(\frac{\partial \tilde{u}}{\partial \tau}\right)_w \tag{2}$$

The boundary conditions on the velocity profile $\tilde{u}(\tilde{x}, \tau)$ are

$$\begin{aligned} \tilde{u}(0, \tau) &= \tilde{u}_j && 0 < \tau < 1 \\ &= 1 && \tau > 1 \\ \tilde{u}(\tilde{x}, 0) &= 0 && \\ \lim_{\tau \to \infty} \tilde{u}(\tilde{x}, \tau) &= 1 && \end{aligned} \tag{3}$$

The accurate representation of such velocity profiles with adequate freedom by means of conventional polynomials would be extremely tedious. Consider profiles generated by an Oseen-type of flow corresponding to $C \equiv 1$, as in Refs. 12 and 13, and take $\tilde{u} = \tilde{u}(\xi, \tau)$ given by a solution to the following "heat conduction" problem:

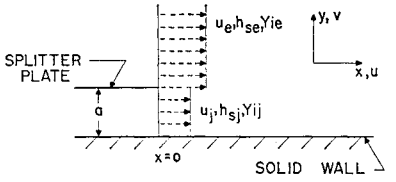

Fig. 1 Schematic representation of a flow field

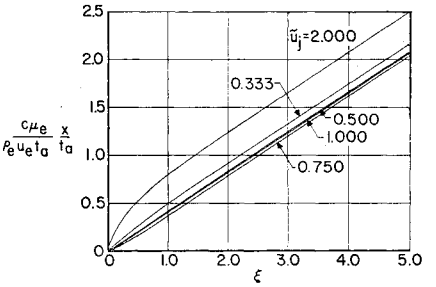

Fig. 2 Evaluation of integral in Eq. (8)

$$\begin{aligned} \partial\tilde{u}/\partial\xi &= \partial^2\tilde{u}/\partial\tau^2 && \\ \tilde{u}(0, \tau) &= \tilde{u}_j && 0 < \tau < 1 \\ &= 1 && \tau > 1 \\ \tilde{u}(\xi, 0) &= 0 && \\ \lim_{\tau\to\infty} \tilde{u}(\xi, \tau) &= 1 && \end{aligned} \tag{4}$$

The variable ξ is considered an unknown function of $\tilde{x}$ determined by satisfying Eq. (2).

The solution of the problem posed by Eq. (4) is[15]

$$\tilde{u}(\xi, \tau) = \tilde{u}_j \operatorname{erf}\left[\frac{\tau}{(4\xi)^{1/2}}\right] + \left(\frac{1 - \tilde{u}_j}{2}\right)\left\{\operatorname{erf}\left[\frac{\tau - 1}{(4\xi)^{1/2}}\right] + \operatorname{erf}\left[\frac{\tau + 1}{(4\xi)^{1/2}}\right]\right\} \tag{5}$$

The wall shear is proportional to $(\partial\tilde{u}/\partial\tau)_w$, which is, from Eq. (5),

$$(\partial\tilde{u}/\partial\tau_w) = (\pi\xi)^{-1/2}[\tilde{u}_j + (1 - \tilde{u}_j)e^{-1/4\xi}] \tag{6}$$

Now for the determination of $\xi = \xi(\tilde{x})$ from Eq. (2), the quantity $(d\tilde{\theta}/d\xi)(\xi)$ is required; this can be evaluated as a function of ξ in closed form. After considerable algebra, there is obtained

$$\begin{aligned} d\tilde{\theta}/d\xi = (2\pi\xi)^{-1/2}\{&\tilde{u}_j{}^2[3 + e^{-1/2\xi} - 4e^{-1/9\xi}] - \tilde{u}_j \times \\ &[2 + 2^{1/2} + 2e^{-1/2\xi} - (2)^{1/2}e^{-1/4\xi} - 4e^{-1/8\xi}] + \\ &(1 + e^{-1/2\xi} - (2)^{1/2}e^{-1/4\xi})\} = (2\pi\xi)^{-1/2}A(\xi) \end{aligned} \tag{7}$$

Substitution of Eqs. (6) and (7) into Eq. (2) results in the following equation yielding implicitly $\xi = \xi(x)$:

$$\frac{\mu_e}{\rho_e u_e t_a}\int_0^x C dx' = \int_0^\xi \frac{A(\xi')d\xi'}{2^{1/2}[\tilde{u}_j + (1 - \tilde{u}_j)e^{-1/4\xi'}]} \tag{8}$$

When a functional form for $C = C(\tilde{x})$ has been chosen, the left-hand side of Eq. (8) can be evaluated. The integral on the right must be evaluated numerically with $\tilde{u}_j$ as a parameter. This has been done for a range of $\tilde{u}_j$ values and $C =$ const, as shown in Fig. 2. It will be noted therefrom that the integral becomes a linear function of ξ for $\xi \gtrsim 1$. As will be discussed in more detail below, this behavior implies that the effect of the defect in the initial profile, $|\tilde{u}_j - 1|$, can be represented by an effective length in the flow direction.

The integrand on the right-hand side of Eq. (8) may be interpreted as an effective velocity $\bar{u}$ nondimensionalized with respect to the external velocity as follows: if the basic partial differential momentum equation for $u = u(x, y)$ is transformed to the variables x and t, there is obtained with $\rho\mu = C\rho_e\mu_e$

$$(u\partial u/\partial x) + \bar{v}(\partial u/\partial t) = C\nu_e(\partial^2 u/\partial t^2)$$

Now, in the spirit of Carrier and Lewis, let

$$(u\partial u/\partial x) + \bar{v}(\partial u/\partial t) \simeq \bar{u}(\partial u/\partial x)$$

and introduce

$$\xi = \int_0^x \left(\frac{C\nu_e}{\bar{u}t_a{}^2}\right) dx'$$

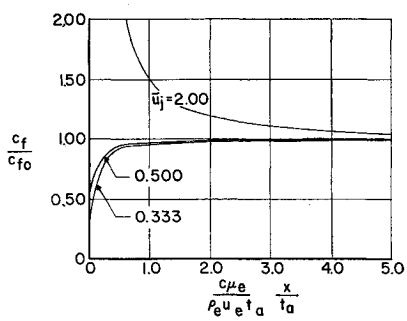

Fig. 3 Variation of skin friction ratio with velocity injection ratio

Then Eq. (4) for $\tilde{u}$ results, and the inverse transformation to the x-t plane can be carried out conveniently according to the equation

$$\left(\frac{\mu_e}{\rho_e u_e t_a}\right)\int_0^{\tilde{x}} C d\tilde{x}' = \int_0^{\xi}\left(\frac{\tilde{u}}{u_e}\right) d\xi' \tag{8a}$$

Now the use of the profiles generated by Eq. (4) in the momentum equation in integral form [Eq. (2)] corresponds to one means for evaluating $(\tilde{u}/u_e)$ in a systematic fashion. Note that comparison of the integrands in Eqs. (8) and (8a) implies, as just stated,

$$\tilde{u}/u_e = A(\xi)/2^{1/2}[\tilde{u}_j + (1 - \tilde{u}_j)e^{-1/4\xi}]$$

Thus, as $\xi \to \infty$, $\tilde{u}/u_e \to (2^{1/2} - 1)$ for all $\tilde{u}_j$.

The results of Figs. 2 indicate that, for all values of $\tilde{u}_j$, reasonable values of $\tilde{u}/u_e$ are obtained so that this approximate technique is not restricted with respect to permissible values of $\tilde{u}_j$.‡

A. Skin-Friction Coefficient

The skin-friction coefficient can be expressed in terms of ξ and thence from Eq. (8) in terms of $\tilde{x}$ with the Reynolds number $(\rho_e u_e t_a/\mu_e)$ as a parameter. There is obtained

$$C_f(\rho_e u_e t_a/C\mu_e) = \{\tilde{u}_j + [(1 - \tilde{u})]e^{-1/4\xi}\}(\pi\xi)^{-1/2} \tag{9}$$

B. Comparison with the Exact Flat Plate Solution

It is interesting to consider the case $\tilde{u}_j = 1$, i.e., a uniform flow at the origin, since the present analysis then provides an approximate solution to the flat plate boundary layer. If C is taken to be constant, then, for $\tilde{u}_j = 1$, Eqs. (8) and (9) yield

$$(C\mu_e/\rho_e u_e t_a)\tilde{x} = (2^{1/2} - 1)\xi \tag{10}$$

and

$$\begin{aligned} C_f(\rho_e u_e x/\mu_e)^{1/2} &= [(2^{1/2} - 1)/\pi]^{1/2} \\ &= 0.363 \end{aligned} \tag{11}$$

Equation (11) should be compared with the exact calculation of Blasius, where the right-hand side equals 0.332; agreement within 10% will be noted.

The result of Eq. (11) can be employed conveniently for the presentation of the skin-friction results for the case C = const in terms of c_f/c_{f0}, the ratio of the skin friction at a given value of $\tilde{x}$ to that which would prevail at the same station if $\tilde{u}_j = 1$. The result is shown in Fig. 3;§ it will be noted therefrom that the effect of the slot in skin-friction persists for a considerable length. For example, if $\rho_e u_e t_a/C\mu_e = 10^3$ and $\tilde{u}_j = \frac{1}{3}$, $C_f/C_{f0} \leq 0.9$ for $x/t_a \lesssim 800$.

‡ Frank Lane has pointed out to the authors that this lack of restriction may not apply to arbitrary initial profiles.

§ A second comparison between this analysis and more exact calculations was attempted; the two-dimensional wall jet was considered. This corresponds to letting $\tilde{u}_j \to \infty$ in Eqs. (5) and (8). It was found that, for all ξ, $\tilde{u}/u_m \simeq 2$, where u_m is the maximum velocity at a given ξ; moreover, for $\xi \to \infty$, the shearing stress at the wall did not have the proper x-dependence. Thus it is concluded that this analysis does not yield accurate results for the wall-jet flow.

III. Analysis for the Distribution of Stagnation Enthalpy

There are considered herein two cases pertaining to the energy equation: those corresponding to an adiabatic wall, and those corresponding to a constant enthalpy wall. For both cases the basic equation is the energy integral corresponding to Eq. (2). For $\sigma = Le = 1$, it may be written

$$\frac{d\tilde{\Omega}}{d\tilde{x}} = \left(\frac{C\mu_e}{\rho_e u_e t_a}\right)\left(\frac{\partial g}{\partial \tau}\right)_w \tag{12}$$

where

$$\tilde{\Omega} = \frac{\Omega}{t_a} = \int_0^{\infty} \tilde{u}(1 - g)d\tau$$

The initial conditions on the distribution of nondimensional stagnation enthalpy $g(x, \tau)$ are

$$\begin{aligned} g(0, \tau) &= g_j & 0 < \tau < 1 \\ &= 1 & \tau > 1 \end{aligned}$$

Moreover, far from the surface

$$\lim_{\tau\to\infty} g(\tilde{x}, \tau) = 1$$

The boundary conditions at $\tau = 0$ change for each case and will be discussed separately.

A. Adiabatic Surface

For the case of zero heat transfer along the surface ($y = 0$), the enthalpy ratio g_w is considered an unknown function of x, but by definition $(\partial g/\partial \tau)_w = 0$. In accordance with the technique used to find an appropriate solution for the velocity field, the profile for g is taken as a solution to the related heat conduction problem with $C \equiv 1$, namely,

$$\partial g/\partial \xi_1 = \partial^2 g/\partial \tau^2 \tag{13}$$

with

$$\begin{aligned} g(0, \tau) &= g_j & 0 < \tau < 1 \\ &= 1 & \tau > 1 \\ \lim_{\tau\to\infty} g(\xi_1, \tau) &= 1 \\ (\partial g/\partial \tau)(\xi_1, 0) &= 0 \end{aligned}$$

Thus

$$g = 1 + \frac{(1 - g_j)}{2}\left[\operatorname{erf}\frac{\tau - 1}{(4\xi_1)^{1/2}} - \operatorname{erf}\frac{\tau + 1}{(4\xi_1)^{1/2}}\right] \tag{14}$$

with $\xi_1 = \xi_1(\tilde{x})$ to be determined from satisfaction of Eq. (12), with the right-hand side set equal to zero. Note that

$$(1 - g_{aw})/(1 - g_j) = \operatorname{erf}[1/(4\xi_1)^{1/2}] \tag{14a}$$

and thus that $g_{aw}(0) = g_j$ and $g_{aw}(\infty) = 1$, as might be expected on physical grounds. It is convenient to retain the differential form of Eq. (12), since in this adiabatic case

$$\frac{d\tilde{\Omega}}{d\tilde{x}} = \left[\frac{\partial\tilde{\Omega}}{\partial\xi} + \frac{\partial\tilde{\Omega}}{\partial\xi_1}\frac{d\xi_1}{d\xi}\right]\frac{d\xi}{d\tilde{x}} = 0 \tag{12a}$$

and since the partial derivatives can be evaluated in closed form.

After considerable analysis, Eq. (12a) leads to the following differential equation:

$$\frac{d\xi_1}{d\xi} = \left(\frac{\xi + \xi_1}{\xi}\right)^{1/2}\frac{[\tilde{u}_j + (1 - \tilde{u}_j)e^{-1/4\xi}]\operatorname{erf}[1/(4\xi_1)^{1/2}]}{B(\xi_1, \xi)} - 1 \tag{15}$$

where

$$B(\xi_1, \xi) = \tilde{u}_j e^{-1/4(\xi+\xi_1)} \operatorname{erf}\{\tfrac{1}{2}[\xi/(\xi_1^2 + \xi\xi_1)]^{1/2}\} + [(1 - \tilde{u}_j)/2][e^{-1/(\xi+\xi_1)} \operatorname{erf}\{\tfrac{1}{2}(\xi - \xi_1) \times [\xi\xi_1(\xi_1 + \xi)]^{-1/2}\} + \operatorname{erf}\{\tfrac{1}{2}[(\xi + \xi_1)/\xi\xi_1]^{1/2}\} \quad (15a)$$

The initial condition on the solution of Eq. (15) is $\xi_1 = 0$ at $\xi = 0$.

An examination of Eqs. (15) and (15a) leads to a limitation of the analysis; it is found that, as $\xi_1, \xi \to 0$, $d\xi_1/d\xi \geq 0$ only for $\frac{1}{3} \leq u_j < 1$. For values of $\tilde{u}_j$ outside this range, ξ_1 is negative; this implies that the representative $\bar{u}$ velocity in the modified Oseen approximation is negative, a physically unappealing result. Moreover, from a mathematical point of view negative values of ξ_1 have drastic consequences with respect to the heat conduction equation. Accordingly, the analysis presented herein is considered to be limited to the forementioned range of $\tilde{u}_j$ values.

Solutions to Eq. (15) for a range of values of $\tilde{u}_j$ have been obtained by numerical integration and are shown in Fig. 4. The Kutta-Runge-Gill method with variable step-size selected according to a curvature criterion was used in conjunction with a Bendix G-15 computer. The results of Figs. 2 and 4 permit the wall enthalpy parameter $(1 - g_{aw})/(1 - g_j)$ to be determined as a function of $\bar{x}$ with $\tilde{u}_j$ as a parameter, as shown in Fig. 5. For the case of homogeneous injection, Fig. 5 permits a complete solution of the energy-temperature fields to be obtained. In particular, g_{aw} is related directly to the wall temperature so that the distribution of adiabatic wall temperature with slot injection can be determined readily with ρ_j/ρ_e, $\tilde{u}_j$, and g_j as parameters.‖ On the other hand, for the heterogeneous case, solution of the species equations is required before the state of the gas can be determined. The species conservation and the chemical models leading thereto will be discussed later.

B. Constant Wall Enthalpy

Consider next the case $g_w = \text{const}$; with some restriction on $\tilde{u}_j$, g_j, and g_w, a Crocco integral exists and provides a simple solution for the energy equation in terms of the velocity $\tilde{u}$. In particular, if

$$g_j = g_w + (1 - g_w)\tilde{u}_j$$

then

$$g = g_w + (1 - g_w)\tilde{u} \quad (16)$$

and the solution for $\tilde{u}(\bar{x}, t)$ leads directly to the solution for the stagnation enthalpy ratio $g(\bar{x}, t)$. Note that in this case there is no limitation on $\tilde{u}_j$.

The heat transfer to the surface for unity Lewis and Prandtl numbers depends only on the gradient of g; thus, Eq. (16) leads to

$$q \equiv \frac{k}{c_p}\frac{\partial h_s}{\partial y}\bigg|_w = -\left(\frac{C\mu e h_{se}}{t_a}\right)(1 - g_w)\left(\frac{\partial \tilde{u}}{\partial \tau}\right)_w$$

Defining a heat transfer coefficient by the relation

$$\mathfrak{h} = \frac{q}{h_w - h_r} \qquad h_r = h_{se} \quad \text{for} \quad \sigma = 1$$

yields

$$Nu \equiv \frac{\mathfrak{h}x}{(k/C_p)_w} = \left(\frac{\rho_w}{\rho_e}\right) C_f Re_x \quad (17)$$

Thus, as with all flows described by a Crocco integral, the heat transfer and skin-friction are related. Equation (17) in conjunction with Fig. 3 also yields q/q_0, where q_0 is the heat transfer flux that would be obtained for $\tilde{u}_j = 1$, as a function of $\tilde{u}_j$. The form of Eq. (17) clearly demonstrates the influence of the jet density upon the heat transfer; light gases tend to alleviate the heat load near the injection point even in the presence of combustion.

‖ The effect of ρ_j/ρ_e enters implicitly through $t_a = (\rho_j/\rho_e)a$.

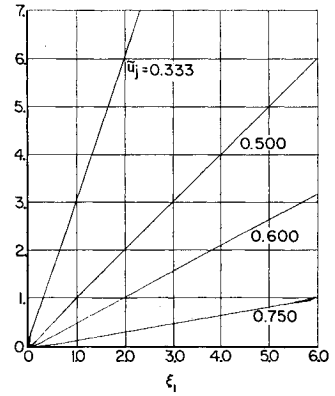

Fig. 4 Relation between energy and momentum variables for adibatic wall

It is reiterated that the surface temperature corresponding to the constant value of g_w is, in the general case of heterogeneous flows, not constant and is unknown until the composition distribution at the wall is determined. Only for the homogeneous case does $g_w = \text{const}$ imply $T_w = \text{const}$.#

IV. Analysis for the Distributions of Composition and State

In the analyses of the previous section the composition of the gas and the models for chemical behavior were inessential.** These aspects will be discussed now; it is necessary first to specify the chemical system under consideration. The injected gas will be taken to be hydrogen and the external stream to be air. Combustion will be assumed to yield only water in gaseous form, and nitrogen will be treated as an inert diluent. It will be convenient for notation to assign numerical subscripts to denote the quantities associated with each species present; thus, let the subscripts 1 to 4 denote oxygen, hydrogen, water, and nitrogen, respectively.

A. Conservation of Element Mass Fractions

With this specification of the chemical system under consideration, it is possible to proceed to the determination of certain features of the composition without the further assumption of a model of chemical behavior. In particular,

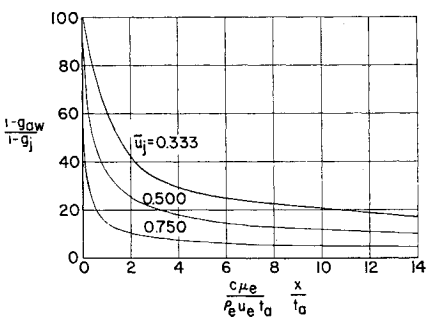

Fig. 5 Variation or adiabatic wall enthalpy parameter

It is pointed out that in the extended version of this paper (General Applied Science Lab. TR-299) the case of constant wall temperature is presented. The same modified Oseen technique as described here is applied in a straightforward manner, although the numerical analysis is considerably more complicated.

** This uncoupling is possible because of the assumption of a uniform external flow and of simplified transport properties ($C \equiv 1$ in the profiles and $\sigma \equiv L_{ei} \equiv 1$).

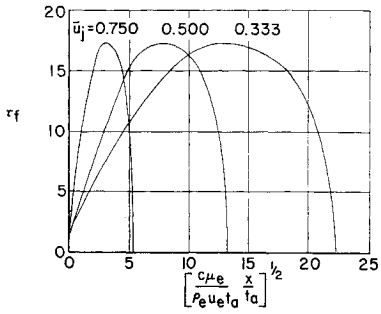

Fig. 6 Configuration of flame sheet

consider the element mass fractions defined by

$$\tilde{Y}_1 = Y_1 + (W_1/2W_3)Y_3$$
$$\tilde{Y}_2 = Y_2 + (W_2/W_3)Y_3 \tag{18}$$

Note that

$$\tilde{Y}_{1_e} = Y_{1e} \qquad \tilde{Y}_{2_e} = 0 \qquad Y_{1_i} = 0 \qquad Y_{2_i} = 1$$

Now at the impermeable surface corresponding to $y = 0$, the diffusional velocities, and thus the normal gradients of the mass fraction of each species, must vanish. Moreover, the same partial differential equation describes g, $\tilde{Y}_1$, $\tilde{Y}_2$, Y_4. Thus, there is a Crocco-type relation between the stagnation enthalpy ratio for the adiabatic wall case and $\tilde{Y}_1$, $\tilde{Y}_2$, and Y_4. Furthermore, the solution for $\xi_1 = \xi_1(\tilde{x})$ given by Eq. (15a) can be employed to yield these mass fractions as functions of $\tilde{x}$ and τ. Accordingly, the same limitation on $\tilde{u}_j$ applies to the solution for the element mass fraction, i.e., $\frac{1}{3} \leq u_j < 1$. The Crocco relations in this case are

$$\tilde{Y}_1 = Y_{1e}(g - g_i)/(1 - g_i) \tag{19}$$
$$\tilde{Y}_2 = (1 - g)/(1 - g_i) \tag{20}$$
$$Y_4 = Y_{4e}(g - g_i)/(1 - g_i) \tag{21}$$

In view of the existing solution for $g(\tilde{x}, \tau)$ given by Eqs. (14) and (15), Eqs. (19–21) provide the distribution of the element mass fractions in terms of $\tilde{x}$ and τ. It should be noted that these solutions apply whether or not the energy solution itself applies to the particular problem at hand. Suppose, for example, the constant g_w case satisfying Eq. (16) is of interest in a particular case; then the element mass fractions are given as functions of $\tilde{x}$ and τ by Eqs. (14, 15, and 19–21) with $(1 - g)/(1 - g_i)$ treated as a parameter to be eliminated so that $\tilde{Y}_i = \tilde{Y}_i(\tilde{x}, \tau)$, $i = 1$, 2, and $Y_4 = Y_4(\tilde{x}, \tau)$ are obtained.

To continue the analysis, a statement concerning the model for chemical behavior must be made. For a diffusing reacting system, one can envision two limiting cases. If initial conditions are such that the reaction proceeds very slowly compared to the diffusion process, the flow field is reaction-controlled. For this case, frozen chemistry may be taken to apply in the mixing region. The statement of the problem is then completed by $Y_3 \equiv 0$, in which case $Y_i = \tilde{Y}_i$ and Eqs. (19–21) yield the complete solution. Indeed this solution applies to the injection of any inert foreign gas through the slot and thus may be of interest, e.g., to the effect of helium injection on skin-friction, adiabatic surface temperature, and heat transfer.

In the second case, the reaction proceeds very rapidly compared to the diffusion process making the system diffusion-controlled. The model of chemical behavior corresponding to this limiting case is local chemical equilibrium in the mixing zone.

B. Flame Sheet Metal

For the limiting case of equilibrium flow, the equilibrium condition relating the concentration of water to that of oxygen and hydrogen provides an additional condition determining the composition. However, as shown in Ref. 18, for the hydrogen-air system with temperatures roughly 2500°K or less, equilibrium flow becomes, for all practical purposes, the flame sheet model widely used in the analysis of boundary layers with chemical reaction.[2,3] This result is due to the magnitude of the equilibrium constant for the foremention temperature range, implying that, at a generic point in the flow, either oxygen or hydrogen or both are present in small amounts. Accordingly, the flame sheet model divides the flow into two regions, one with no oxygen present and the other with no hydrogen present. Combustion takes place at and water diffuses from the interface between these two regions.

It should be recognized that the assumption of a flame sheet model, being related to an equilibrium chemical behavior, is a further idealization in the analysis, albeit one frequently employed. In the present case, the model is of practical utility when the static temperature is high with moderate static pressures (e.g., 1000°K, 0.05 atm).

Consider the determination of the location of the flame sheet in the $\tilde{x}$-τ plane, i.e., $\tau = \tau_f = \tau_f(\tilde{x})$. At the flame sheet $Y_1 = Y_{1f} = 0$ and $Y_2 = Y_{2f} = 0$, so that

$$\tilde{Y}_{1f} = (W_2/2W_3)Y_{3f} \tag{22}$$
$$\tilde{Y}_{2f} = (W_2/W_3)Y_{3f} \tag{23}$$

Now if Eq. (14) is substituted into Eq. (20), and Eqs. (22) and (23) are considered, there results

$$\operatorname{erf}\left(\frac{\tau_f - 1}{4\xi_1}\right) - \operatorname{erf}\left(\frac{\tau_f + 1}{4\xi_1}\right) = -\frac{4W_2Y_{1e}}{W_1 + 2W_2Y_{1e}} \tag{24}$$

which defines $\tau_f = \tau_f(\xi_1)$; with $\xi_1(\tilde{x})$ known from the solution of Eq. (15), the desired results for the location of the flame sheet are obtained. Of particular interest will be the point of impingement of the sheet on the surface ($\tau_f = 0$), since this determines the length required to consume all the hydrogen and the location of high heat transfer rates or of high adiabatic surface temperatures; this location is defined by $\tau_f = 0$; denote the corresponding value of $\xi_1 = \xi_{1f}$. Then from Eq. (29), ξ_{1f} is defined by

$$\operatorname{erf}\frac{1}{(4\xi_{1f})^{1/2}} = \frac{2W_2Y_{1e}}{W_1 + 2W_2Y_{1e}} \tag{25}$$

Thus from Eq. (25) and the solution of Eq. (15), the value of $\tilde{x}$ corresponding to ξ_{1f} can be found; note that this $\tilde{x}$ depends only on $\tilde{u}_j$. In Fig. 6 the shapes of the flame sheet $\tau_f = \tau_f(\tilde{x})$ for various injection rates $\tilde{u}_j$ are shown. It is interesting to note therefrom that the $\tilde{x}$-length for total consumption of the hydrogen decreases as $\tilde{u}_j$ increases. This would appear to be related to the increased shear and therefore increased diffusion as $\tilde{u}_j$ increases and is in contradistinction to the results for turbulent free mixing in Ref. 16.

With the location of the flame sheet established, the entire distribution of composition can be determined. At a given station defined by ξ_1, Eqs. (19–21) are supplemented by the statements that, for $\tau < \tau_f$, $Y_1 = 0$, and for $\tau > \tau_f$, $Y_2 = 0$. The composition along the wall can be found in a similar fashion since, for $\xi_1 < \xi_{1f}$, $Y_{1w} = 0$, and for $\xi_1 > \xi_{1f}$, $Y_{2w} = 0$. The wall distributions of composition are shown in Fig. 7 in terms of ξ_1.

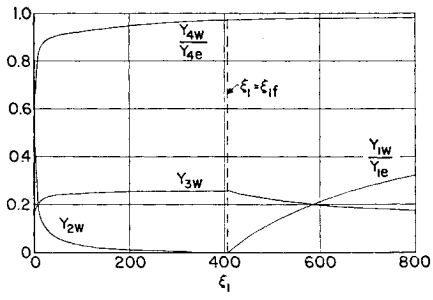

Fig. 7 Distribution of wall composition

C. Temperature and Density Distributions

Assume now that the stagnation enthalpy distribution for a particular problem is known; then the composition distribution, obtained as in the foregoing, can be used in conjunction therewith to obtain the temperature distribution. For this purpose it is convenient and sufficiently accurate for most purposes to take

$$h_i = \Delta_i + \bar{C}_{pi}(T - T_r) \tag{26}$$

Then

$$\Theta \equiv \frac{T - T_r}{T_e - T_r} = \frac{gh_{se} - \Sigma\, Y_i\Delta_i - (u_e^2/2)\tilde{u}^2}{(T_e - T_r)\,\Sigma\, Y_i C_{pi}} \tag{27}$$

Furthermore, the density ratio is required for the inverse transformation corresponding to Eq. (1); it is given by

$$\frac{\rho_e}{\rho} = \frac{T}{T_e}\frac{W_e}{W} = \frac{W_e}{W}\left[\Theta + (1 - \Theta)\frac{T_r}{T_e}\right] \tag{28}$$

where

$$W^{-1} = \sum_i \frac{Y_i}{W_i}$$

Note that

$$\bar{y} = \frac{y}{t_a} = \int_0^\tau \frac{\rho_e}{\rho}\, d\tau'$$

$$= W_e \int_0^\tau \frac{1}{W}\left[\Theta + (1 - \Theta)\frac{T_r}{T_e}\right] d\tau' \tag{29}$$

V. Numerical Example

As an example of the application of the foregoing analysis, some numerical results are given here for typical conditions pertinent to the problem of the combustion of gaseous hydrogen boiloff which is vented from the upper stages of a large rocket booster. Initial conditions on the freestream are taken as a static temperature of 1000°K, a static pressure of 0.05 atm, and a velocity of 4300 fps. The vented hydrogen is taken at a static temperature of 380°K, a static pressure of 0.05 atm, and a velocity of 2150 fps. The supersonic boundary layer on the splitter plate will contain a small quantity of very high static temperature air near the wall as a result of the effects of viscous dissipation. This air makes the first contact with the hydrogen and will ignite almost instantly due to its high static temperature. This small reaction zone consequently will trigger the combustion of the main air stream with the hydrogen jet, resulting in a rapid diffusion-controlled combustion process that can be studied by the analysis considered herein.

The thermal boundary condition taken is that of an adiabatic wall. Thus the distribution of wall enthalpy is determined from Fig. 5. With Figs. 7, 4, and 2, this may be transformed into a distribution of adiabatic wall temperature with the physical streamwise coordinate x for any given slot height. The results of this operation are shown in Fig. 8 for a slot height of 0.02 ft. It may be observed that the effect of combustion is felt at the wall within a distance of only 2 ft and that thereafter the wall temperature rises very rapidly, reaching a value of 2300°K in 100 ft. It is important, however, to note that at 100 ft the wall still is being cooled compared to the recovery temperature of the freestream (2500°K), even in the presence of combustion.

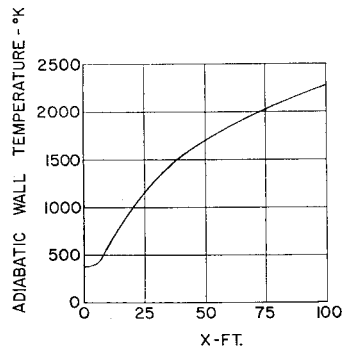

Fig. 8 Adiabatic wall temperature distribution for numerical example

References

[1] Lees, L., "Convective heat transfer with mass addition and chemical reactions," *Combustion and Propulsion, Third AGARD Colloquium* (Pergamon Press, New York, 1959), pp. 451–499.

[2] Cohen, C. B., Bromberg, R., and Lipkis, R. P., "Boundary layer with chemical reaction due to mass addition," Jet Propulsion **28**, 659–668 (1958).

[3] Eschenroeder, A. Q., "Combustion in the boundary layer on a porous surface," J. Aerospace Sci. **27**, 901–906 (1960).

[4] Ferri, A., "Possible directions of future research in air-breathing engines," *Combustion and Propulsion, Fourth AGARD Colloquium* (Pergamon Press, New York, 1960), pp. 3–15.

[5] Flugge-Lotz, I., "A Difference method for the computation of the laminar compressible boundary layer." *50 Jahre Grenzschichtforschung* (Frederick Vieweg and Sohn, Braunschweig, 1955), p. 393.

[6] Howe, J., "Some finite difference solutions of the laminar compressible boundary layer showing the effects of upstream transpiration cooling," NASA Memo. 2-26-59A (February 1959).

[7] Kramer, R. F. and Lieberstein, H. M., "Numerical solution of the boundary layer equations without similarity assumptions," J. Aerospace Sci. **26**, 508–514 (1959).

[8] Pallone, A., "Non-similar solutions of the compressible laminar boundary layer equations with applications to the upstream transpiration cooling problem," J. Aerospace Sci. **28**, 449–456 (1961).

[9] Libby, P. A. and Pallone, A., "A method for analyzing the insulating properties of the laminar compressible boundary layer," J. Aeronaut. Sci. **21**, 825–834 (1954).

[10] Rubesin, M. W. and Inouye, M., "A theoretical study of the effect of upstream transformation-cooling on the heat-transfer and skin friction characteristics of a compressible, laminar boundary layer," NACA TN 3969 (May 1957).

[11] Cresci, R. J., "Theoretical analysis of the downstream influence of stagnation point mass transfer," Wright Air Dev. Div. TR-60-434 (June 1961); also Internatl. J. Heat Mass Transfer (to be published).

[12] Lewis, J. A. and Carrier, G. F., "Some remarks on the flat plate boundary layer," Quart. Appl. Math. **7**, 228–234 (1949).

[13] Carrier, G. F., "On the integration of equations associated with problems involving convection and diffusion," *Tenth International Congress of Theoretical and Applied Mechanics, Stresa, Italy* (Elsevier Publishing Co., Amsterdam, 1960).

[14] Chapman, D. R. and Rubesin, M. W., "Temperature and velocity profiles in the compressible laminar boundary layer with arbitrary distribution of surface temperature," J. Aeronaut. Sci. **16**, 547–565 (1949).

[15] Carslaw, H. S. and Jaeger, J. C., *Conduction of Heat in Solids* (Oxford University Press, New York, 1959), 2nd ed., Chap. II.

[16] Libby, P. A., "Theoretical analysis of turbulent mixing of reactive gases with application to supersonic combustion of hydrogen," ARS J. **32**, 388–396 (1962).